LETTER

Influence of defects and doping on phonon transport properties of monolayer $MoSe_2$

To cite this article: Zhequan Yan *et al* 2018 *2D Mater.* **5** 031008

2D Materials

RECEIVED
10 January 2018

REVISED
28 March 2018

ACCEPTED FOR PUBLICATION
11 April 2018

PUBLISHED
30 April 2018

LETTER

Influence of defects and doping on phonon transport properties of monolayer $MoSe_2$

Zhequan Yan[1], Mina Yoon[2,3] and Satish Kumar[1]

[1] G.W. Woodruff School of Mechanical Engineering, Georgia Institute of Technology, Atlanta, GA, United States of America
[2] Oak Ridge National Laboratory, Center for Nanophase Materials Sciences, Oak Ridge, TN, United States of America
[3] Department of Physics and Astronomy, University of Tennessee, Knoxville, TN 37916, United States of America

E-mail: satish.kumar@me.gatech.edu

Keywords: density functional theory, phonon BTE, defects, doping, thermal conductivity

Supplementary material for this article is available online

Abstract

The doping of monolayer $MoSe_2$ by tungsten (W) can suppress the Se vacancy concentration, but how doping and resulting change in defect concentration can tune its thermal properties is not understood yet. We use first-principles density functional theory (DFT) along with the phonon Boltzmann transport equation (BTE) to study the phonon transport properties of pristine $MoSe_2$ and W doped $MoSe_2$ with and without the presence of Se vacancies. We found that for samples without Se vacancy, the W doping could enhance the thermal transport of monolayer $MoSe_2$ due to reduced three-phonon scattering phase space. For example, we observed that the 16.7% W doping increases the thermal conductivity of the monolayer $MoSe_2$ with 2% Se vacancy by 80% if all vacancies can be suppressed by W-doping. However, the W doping in the defective $MoSe_2$ amplifies the influence of the phonon scattering caused by the Se vacancies, which results in a further decrease in thermal conductivity of monolayer $MoSe_2$ with defects. This is found to be related with higher phonon density of states of $Mo_{0.83}W_{0.17}Se_2$ and larger mass difference between W and Se atoms compared to Mo and Se atoms. This study deciphers the effect of defects and doping on the thermal conductivity of monolayer $MoSe_2$, which helps us understand the mechanism of defect-induced phonon transport, and provides insights into enhancing the heat dissipation in $MoSe_2$-based electronic devices.

$MoSe_2$ as one of the two-dimensional (2D) ultrathin transition metal dichalcogenides (TMDCs) emerged as a promising alternative of graphene for nano-electronic and opto-electronic devices [1–6]. It exhibits unique electronic and optical properties such as an intrinsic band gap [7–10], strong photoluminescence (PL) [11] and efficient photovoltaic (PV) response [12, 13]. In contrast to an indirect gap ~1.1 eV in bulk $MoSe_2$, the monolayer $MoSe_2$ exhibits direct bandgap of ~1.55 eV [7]. The unique electronic/optical properties and atomic-thickness make it promising for flexible nano-electronic applications such as switchable transistors [11, 14], photodetectors [12], ultrathin PV devices [10, 13], as well as thermoelectric applications [15, 16]. In addition, ultra-thin nanosheets of $MoSe_2$ show a room-temperature mobility of ~50 $cm^2\ V^{-1}\ s^{-1}$ [14], which increases almost four-fold when the temperature decreases to 78 K. Therefore, the monolayer $MoSe_2$ becomes the promising material in next-generation ultrathin nano-electronic devices. However, inefficient thermal management may become challenging for the performance and reliability of ultrathin nano-electronic devices as the device dimension scales down and power increases. Phonons are expected to be the dominant energy carriers for the thermal transport in 2D TMDs [6, 17–19]. A fundamental understanding of phonon transport properties of the monolayer $MoSe_2$ is of great importance for improving reliability and energy efficiency of the $MoSe_2$-based devices. A recent theoretical study reported a relatively low thermal conductivity of monolayer $MoSe_2$ (54 W mK^{-1} at room temperature) compared to other 2D TMDs by solving Peierls–Boltzmann transport equation (PBTE) calculations [17]. A much lower thermal conductivity of 17.6 W mK^{-18} is obtained using Slack model [20, 21]. In addition, due to the imperfection of growth processes, the crystal lattice

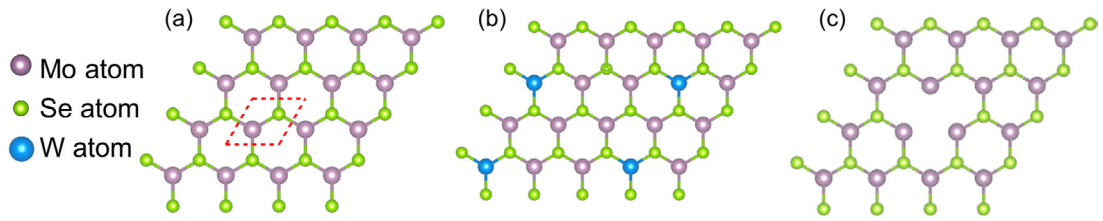

Figure 1. Top view of the structure of (a) monolayer $MoSe_2$, (b) W doped monolayer $MoSe_2$, (c) monolayer $MoSe_2$ with Se vancancies (schematic). The purple, green, and blue spheres represent molybdenum, selenium, and tungsten atoms, respectively.

of monolayer TMDs contains unintentional localized defects such as vacancies [22–26], dislocation cores and grain boundaries [27] which could further suppress the thermal transport [28, 29]. Peng *et al* found that the defect-induced quasi-localized phonon states have a significant influence on reducing the thermal conductivity of MoS_2 from the first-principles calculations [28]. Ding *et al* used non-equilibrium molecular dynamics simulations to demonstrate that thermal conductivity of monolayer MoS_2 can be effectively tuned by introducing phonon–defect scattering [29]. However, very few studies has focused on exploring the effect of defects on the thermal transport in monolayer $MoSe_2$. The defect engineering for Selenium vacancies in the monolayer $MoSe_2$ can provide promising opportunities for tailoring its properties for various device applications [30–32]. Isoelectronic doping is one of the most effective strategies to suppress or to manage the vacancy concentration [33] and precisely tailor its properties for desired applications, such as enhancing the PL, modulating the carrier type and raising the carrier lifetime [23–25, 34]. Azizi, *et al* found that the triangular monolayer flakes of $W_xMo_{1-x}S_2$ ($x \sim 0.5$) is electronically isotropic but vibrationally anisotropic due to the nearly identical electronic properties but very different atomic masses of Mo and W [35]. However, the understanding of the effects of isoelectronic doping process on the thermal transport properties of monolayer $MoSe_2$ is far from being completed.

In this letter, we use first-principle density functional theory (DFT) along with the phonon Boltzmann transport equation (BTE) to study the phonon transport properties of monolayer $MoSe_2$ considering the effects of scattering by the boundary, defects, and doping. The effect of sample size on thermal conductivity at different temperatures is studied along with the influence of Se vacancies. The model for estimating the effect of Se vacancies on phonon properties of the monolayer $MoSe_2$ is developed by considering contributions of two different types of the defect-induced phonon scatterings: one caused by the missing mass of the Se atoms, the other caused by the change of force constants between the under-coordinated atoms near the vacancies. To further illustrate how the Se vacancies affect the phonon transport in the monolayer $MoSe_2$ meanwhile suppressing the Se vacancy concentration, we investigate the phonon property of the monolayer $MoSe_2$ with 16.7% W doping. This percentage W doping is selected for the present study because samples with such percentage of doping has been fabricated and Se vacancy suppression has been demonstrated in [24, 36]. We find that the W doping could enhance the thermal transport of the pristine monolayer $MoSe_2$ if the boundary scattering is ignored, i.e. for large size samples. However, the W doping in the defective $MoSe_2$ amplifies the influence of the phonon scattering caused by the Se vacancies, which results in a further decrease in thermal conductivity of monolayer $MoSe_2$ with Se vacancies.

Total energy calculations are based on the first-principles DFT as implemented in the Vienna *ab initio* simulation package (VASP) [37]. A plane-wave basis set and the projector augmented-wave (PAW) method are used with Perdew, Burke, and Ernzerhof (PBE) exchange-correlation functional [38–40]. The kinetic energy cutoff of the supercell is 500 eV. The system energy convergence criterion is set to be 10^{-9} eV. The force convergence criterion is set to be -0.01 eV $Å^{-1}$. The structure of monolayer $MoSe_2$ shown in figure 1(a) is optimized with an $18 \times 18 \times 1$ grid for Brillouin zone sampling. An 18 Å vacuum space along the *z*-axis is used to eliminate the interaction emerging from the periodic boundary condition. The lattice constant of the monolayer $MoSe_2$ is obtained with the value of 3.32 Å, which is in good agreement with the theoretical result of 3.32 Å [17], and the experimental result of 3.30 Å [41]. Using this optimized lattice constant, the 6×6 and 4×4 supercells of monolayer $MoSe_2$ with $3 \times 3 \times 1$ k-point grid are assembled for the calculations of the second-order harmonic and third-order anharmonic interatomic force constants (IFCs), respectively. The displacement length of each atom from its equilibrium position is 0.01 Å. The interactions between atoms up to the 4th nearest neighboring shell are taken into account for the third-order IFCs calculation. Using the second-order and third-order IFCs obtained from the first-principles calculations, the phonon relaxation times and thermal conductivities of monolayer $MoSe_2$ can be calculated using Fermi's Golden rule [42] with the relaxation time approximation (RTA) and the iterative solution of the BTE [19, 43–45] (see section A in the supporting information (stacks.iop.org/TDM/5/031008/mmedia)). In addition, following the Matthiessen's

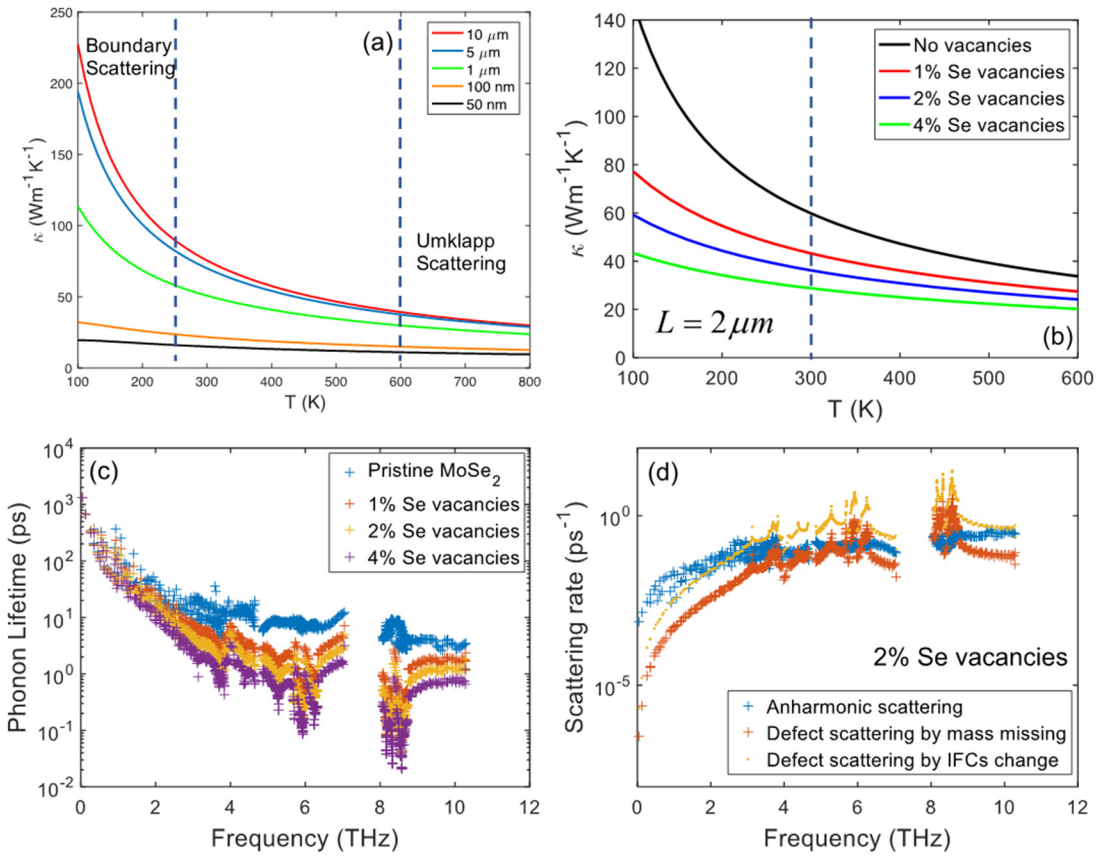

Figure 2. (a) Size-dependent thermal conductivity of monolayer $MoSe_2$ as a function of temperature. (b) Temperature-dependent thermal conductivity of monolayer $MoSe_2$ with Se vacancies. The sample size is 2 μm. (c) Angular frequency dependent phonon lifetime of monolayer $MoSe_2$ with Se vacancies at 300 K. (d) Anharmonic and two types of defect-induced phonon scattering rates (due to mass missing and IFC change) of monolayer $MoSe_2$ with 2% Se vacancies.

rule [46] we calculate the size-dependent thermal conductivity at different temperatures by combining the phonon scattering due to anharmonicity and size effect [47, 48]. Furthermore, we consider the effects of Se vacancies in the monolayer $MoSe_2$ on the phonon scattering rate and thermal conductivity by adding two different types of the defect-induced phonon scattering to the total phonon scattering rate:

$$1/\tau = 1/\tau_{anh} + 1/\tau_b + 1/\tau_V + 1/\tau_F \quad (1)$$

where $1/\tau_{anh}$ and $1/\tau_b$ are the intrinsic anharmonic phonon scattering rate and phonon boundary scatting rate, respectively. $1/\tau_V$ is the scattering rate caused by the missing mass of the Se atom in the crystal, and $1/\tau_F$ is the scattering rate caused by the change of force constants between the under-coordinated atoms near the vacancies. They can be expressed as [49–52],

$$1/\tau_V = x(-\frac{M_V}{M} - 2)^2 \frac{\pi}{2} \frac{\omega^2 g(\omega)}{G} \quad (2)$$

$$1/\tau_F = x(\frac{\delta C}{C})^2 4\pi \frac{\omega^2 g(\omega)}{G} \quad (3)$$

where x is the density of vacancies, M is the average mass per atom, M_V is the mass of the missing atom, $g(\omega)$ is the phonon density of states (DOSs), G is the number of atoms in the crystal and C is the force constant.

Figure 2(a) presents the size-dependent thermal conductivity of monolayer $MoSe_2$ at different temperatures. Results show that the phonon boundary scattering has a significant influence on the thermal conductivity if the sample size is smaller than 1 μm. Below that size, most of the phonons will have a higher probability to hit the boundary before they scatter with other phonons [19]. While the size effect can be ignored if the sample size is larger than 10 μm since the maximum phonon mean free path in $MoSe_2$ is around 10 μm. Furthermore, the boundary effects also play a significant role in the thermal conductivity at the low temperature. It is because the strength of the Umklapp three-phonon process [53] at low temperatures is relatively weak and the phonon boundary scattering becomes much more dominant in the phonon transport process. On the other hand, at high temperatures (>800 K), the size effect can be ignored because the phonon transport is dominated by the strong Umklapp process.

Besides the boundary effects, defects also have a significant impact on the thermal conductivity of monolayer $MoSe_2$. Figures 2(b) and (c) shows the temperature-dependent thermal conductivity and phonon lifetime of monolayer $MoSe_2$ with Se vacancies. The calculations are based on the sample size of 2 μm. Results indicate that 1%, 2% and 4% Se

vacancies decrease the thermal conductivity of monolayer $MoSe_2$ by 27.7%, 39.5% and 51.9%, respectively at room temperature. In our model (equations (2) and (3)), the effect of Se vacancies in crystals on phonon transport is treated by perturbation theory, i.e., contribution to the phonon scattering rate by two different types of the defect-induced phonon scatterings. One corresponds to the missing mass of the Se atoms, which implies the removal of the kinetic energy and potential energy. The other corresponds to the change of force constants between the under-coordinated atoms near the vacancies. Both of these defect-induced phonon scattering increase the total phonon scattering rate and decrease the phonon lifetime in the entire frequency range (figure 2(c)). Furthermore, we also find that the defect-induced phonon scattering rate caused by the change of the force constants near the vacancies has more impact on the total thermal conductivity than that caused by the atom mass missing as shown in figure 2(d). We observe that Se vacancies have a weak impact on the thermal conductivity at high temperatures. It is because that the three-phonon scattering rates corresponding to anharmonicity become dominant at high temperatures and the scattering rates corresponding to the defect related terms, $1/\tau_V$ and $1/\tau_F$ in equation (1), have less contribution to the total phonon scattering rate.

In order to understand the influence of methods to suppress the defect concentration in the monolayer $MoSe_2$, we study the phonon transport property of $MoSe_2$ under the influence of the W doping. The structure of the W doped monolayer $MoSe_2$ used in this work is shown in figure 1(b), which is optimized with the same lattice constant as of monolayer $MoSe_2$. The concentration of W atoms is about 16.7%, which makes the W doped $MoSe_2$ as $Mo_{0.83}W_{0.17}Se_2$. The 2×2 supercell of monolayer $MoSe_2$ is assembled for the calculations of the second-order harmonic and third-order anharmonic IFCs. Figure 3(a) shows the temperature-dependent thermal conductivity of monolayer pristine $MoSe_2$ and W doped $MoSe_2$ with various sample sizes. We find that the W doping increases the thermal conductivity of monolayer pristine $MoSe_2$. In addition, the difference becomes larger as the temperature increases (figure 3(a)). To better understand the impact of W doping on the thermal conductivity of the pristine $MoSe_2$, we also calculated the size-dependent thermal conductivity of the monolayer $MoSe_2$ and the W doped $MoSe_2$,which is compared to that of the monolayer WSe_2 at 300 K (figure 3(b)). Results indicate that the thermal conductivity of W doped $MoSe_2$ is similar to that of the pristine $MoSe_2$ for sample sizes smaller than 1 μm. The phonon scattering from boundary effect has a greater impact on the thermal conductivity of the W doped $MoSe_2$ than that of the pristine $MoSe_2$. If we reduce the boundary scattering influence by considering large-size samples, the W doping could increase the thermal conductivity of pristine $MoSe_2$, e.g., 23.6% increase is observed for 10 μm sample (figure 3(b)). This indicates that for low sample size, boundary scattering effect is significant leading to similar conductivity but the intrinsic thermal conductivity of W doped $MoSe_2$ is higher than pristine $MoSe_2$ as observed in large-size samples.

To further understand it, we calculate the phonon dispersions of monolayer $MoSe_2$ and WSe_2 along $\Gamma - M$ direction which is shown in figure 4(a). As expected, all the phonon branches of WSe_2 are lower in frequency than that of $MoSe_2$ because of the mass difference between W and Mo atoms. In addition, a larger gap between the optical and acoustic phonon branches in WSe_2 (1.3 THz) is observed than that in $MoSe_2$ (0.21 THz). Due to the larger gap between optical and acoustic phonon branches of WSe_2, more energy is needed for the annihilation process of two acoustic phonon modes into one optical mode in WSe_2. As a result, probability of this type of phonon scatterings becomes less leading to the decrease of the Umklapp scattering strength in WSe_2 compared to the $MoSe_2$. Therefore, the thermal conductivity of the monolayer WSe_2 is larger than that of the monolayer $MoSe_2$. Introducing W atoms in the $MoSe_2$ results in thermal conductivity values between that of $MoSe_2$ and WSe_2. Furthermore, it can also be supported by the three-phonon scattering phase space in figure 4(b). It indicates the volume of phase space available for three-phonon scattering, which is another way to indicate the likelihood of phonons being scattered. The details of calculation are provided in the section B of the supporting information. The phase space of the monolayer $MoSe_2$ is larger than that of the $Mo_{0.83}W_{0.17}Se_2$ as expected from the smaller phonon frequency gap between optical and acoustic branches (figure 4(b)). In other words, the phonons in $Mo_{0.83}W_{0.17}Se_2$ will have fewer channels for three-phonon scatterings, which results in the relatively longer phonon relaxation time (figure 5(b)) and larger thermal conductivity.

What happens to the thermal conductivity of the monolayer $MoSe_2$ if there still exist defects such as Se vacancies after the W doping? In order to investigate the impact of the defects on the thermal conductivity of the W doped $MoSe_2$, we calculate the temperature-dependent thermal conductivity and phonon lifetime of the W doped $MoSe_2$ with Se vacancies (figures 5(a) and (b)). Results indicate that after 16.7% W doping, the existence of 1%, and 2% Se vacancy concentration decreases the thermal conductivity of the monolayer $MoSe_2$ by 34.0%, and 46.2%, respectively, at room temperature. Compared with the 27.7%, and 39.4% decrease of the thermal conductivity of monolayer $MoSe_2$ with the same Se vacancy concentration, we find that the introduction of W atoms in the defective $MoSe_2$ amplifies the influence of the phonon scattering caused by the Se vacancies, which results in a further decrease in thermal conductivity compared to that of monolayer $MoSe_2$ with defects. For example, the W doping suppresses the Se-vacant sites by 50% (from 4% to 2%). The thermal conductivity of the 2%

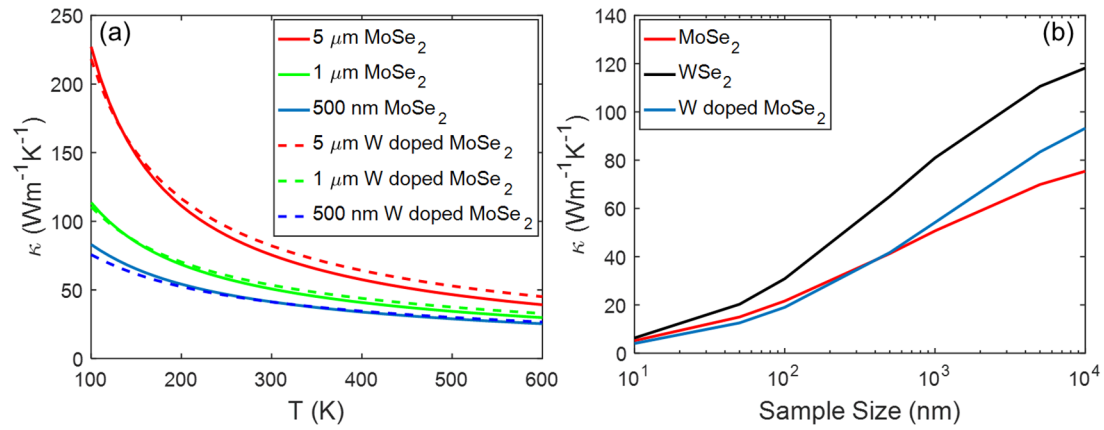

Figure 3. (a) Temperature-dependent thermal conductivity of monolayer pristine $MoSe_2$ and W doped $MoSe_2$ with various sample sizes. (b) Effect of sample size on the thermal conductivity of monolayer pristine $MoSe_2$, WSe_2 and W doped $MoSe_2$ (16.7%), i.e. $Mo_{0.83}W_{0.17}Se_2$ at 300 K.

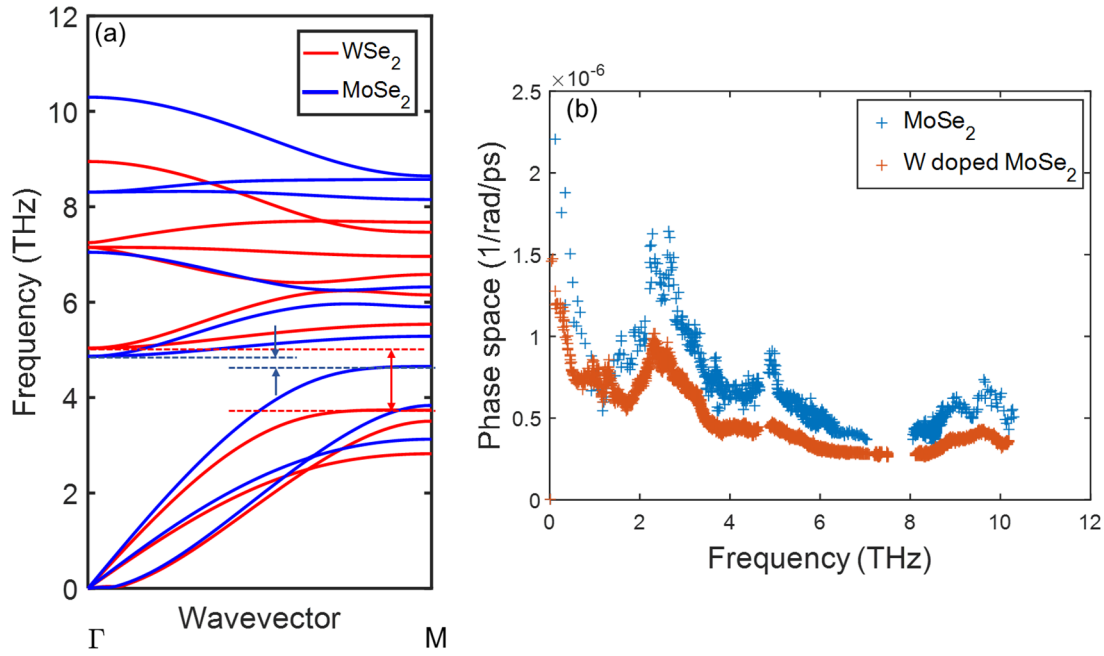

Figure 4. (a) Phonon dispersions of monolayer $MoSe_2$ and WSe_2 along $\Gamma - M$ direction. The gap between the acoustic modes and optical modes are marked in the figure. (b) Three-phonon scattering phase space of monolayer $MoSe_2$ and $Mo_{0.83}W_{0.17}Se_2$.

defective W doped $MoSe_2$ is just 1.4% higher than that of 4% defective monolayer $MoSe_2$, figure 5(a). However, if the doping process makes the 2% Se-vacant $MoSe_2$ into the W doped $MoSe_2$ with no Se vacancies, the thermal conductivity can be increased dramatically by more than 80%.

To further illustrate why the introduced defects amplify the influence of the phonon scattering in the W doped $MoSe_2$, we investigate the phonon DOSs of the monolayer pristine $MoSe_2$ and $Mo_{0.83}W_{0.17}Se_2$ (figure 5(c)). We find that in the low-frequency range, the DOSs of the $Mo_{0.83}W_{0.17}Se_2$ is larger than those of the $MoSe_2$. Due to the correlation between the phonon DOSs and the defect-induced phonon scattering rate as shown in equations (2) and (3), the defect-induced phonon scatterings of the W doped $MoSe_2$ would have more impact on the thermal conductivity than that of the monolayer $MoSe_2$. In addition, we noticed that the $Mo_{0.83}W_{0.17}Se_2$ generates a new peak of DOSs at around 7.5 THz. However, this new peak of DOSs has a very limited contribution to the thermal conductivity because the group velocities of phonons around the 7.5 THz frequency are almost zero. Another explanation of how the introduced Se vacancies amplify the influence of the phonon scattering in W doped $MoSe_2$ is the mass difference between the W and Mo atoms. Since the mass of the W atom is larger than that of the Mo atom, the missing Se atom at a vacancy site results in a larger mass difference (compared to the average mass of the cell), which results in the larger kinetic energy and potential energy change. It enhances the defect-induced phonon scatterings and results in the further suppression of the thermal conductivity of the W doped $MoSe_2$.

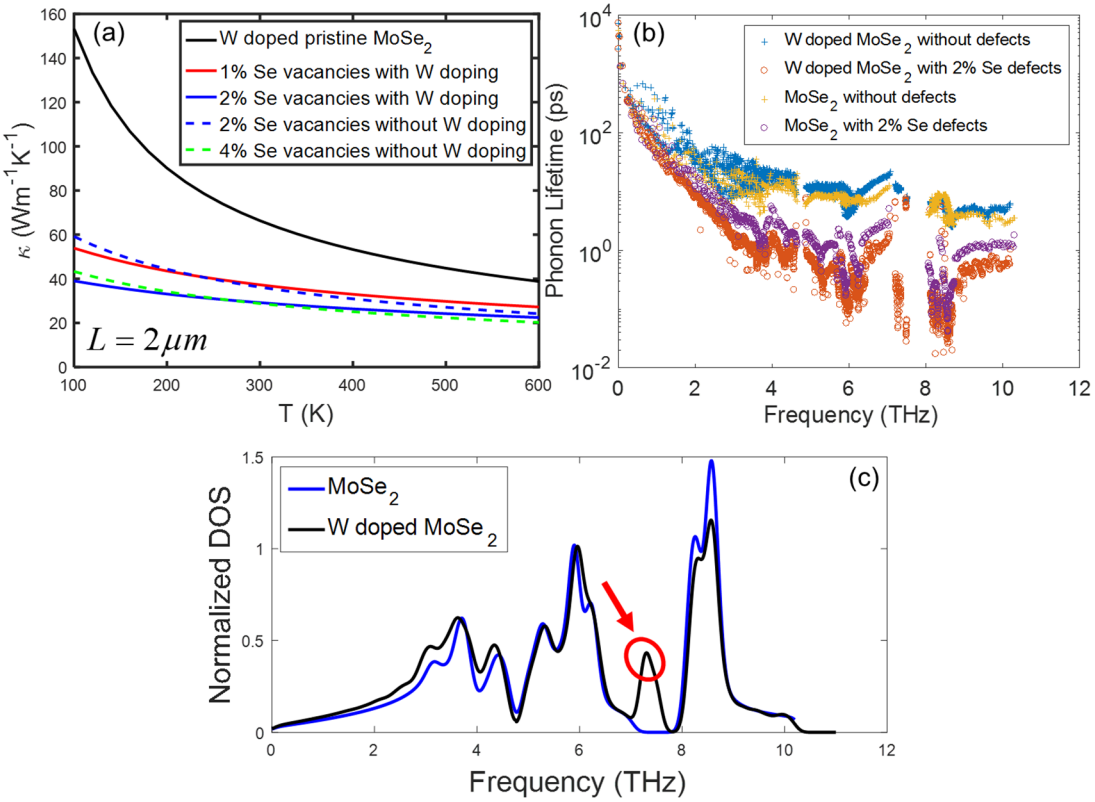

Figure 5. (a) Temperature-dependent thermal conductivity of W doped $MoSe_2$ with Se vacancies. The sample size is 2 μm. (b) Phonon lifetime of monolayer $MoSe_2$ and W doped $MoSe_2$ with or without Se vacancies at 300 K. (c) Phonon DOSs of monolayer $MoSe_2$ and W doped $MoSe_2$.

Conclusion

In conclusion, we investigate the role of size, defects and W doping on thermal conductivity of monolayer $MoSe_2$ by the first principles calculation and the phonon Boltzmann transport equation. We find that 1%, 2% and 4% Se vacancies decrease the thermal conductivity of monolayer $MoSe_2$ of size 2 μm by 27.7%, 39.5% and 51.9%, respectively at the room temperature. However, 16.7% W doping could enhance the thermal transport of the monolayer $MoSe_2$ with 2% Se vacancy by 80% if all vacancies can be suppressed by W-doping, which could be explained by the fewer three-phonon scattering phase spaces of $Mo_{0.83}W_{0.17}Se_2$ and could also be supported by the larger gap between the optical and acoustic phonon branches in WSe_2 than that in $MoSe_2$. However, the W doping in the defective $MoSe_2$ amplifies the influence of the phonon scattering caused by the Se vacancies, which results in a further decrease in thermal conductivity due to the higher phonon DOSs of $Mo_{0.83}W_{0.17}Se_2$ and larger mass difference between W and Se atoms compared to Mo and Se atoms. Results indicate that for 16.7% W doping, the existence of 1%, and 2% Se vacancy concentration decreases the thermal conductivity of the monolayer $MoSe_2$ by 34.0%, and 46.2%, respectively, at the room temperature. The results from this work will help to understand the phonon transport properties of monolayer $MoSe_2$ under the influence of defects and doping, and provide insights for the future design of $MoSe_2$-based electronics.

Acknowledgments

This work was partially supported by the National Science Foundation Grant CBET-1236416. Part of this research was conducted at the Center for Nanophase Materials Sciences, which is a DOE Office of Science User Facility and supported by Creative Materials Discovery Program through the National Research Foundation of Korea (NRF) funded by the Ministry of Science, ICT and Future Planning (NRF-2016M3D1A1919181). This research used the resources of the National Energy Research Scientific Computing Center, a DOE Office of Science User Facility supported by the Office of Science of the US Department of Energy under the Contract No. DE-AC02- 05CH11231.

ORCID iDs

Zhequan Yan https://orcid.org/0000-0001-8026-0264

References

[1] Ataca C, Sahin H and Ciraci S 2012 *J. Phys. Chem.* C **116** 8983–99

[2] Lee Y-H, Yu L, Wang H, Fang W, Ling X, Shi Y, Lin C-T, Huang J-K, Chang M-T and Chang C-S 2013 *Nano Lett.* **13** 1852–7
[3] Tonndorf P, Schmidt R, Böttger P, Zhang X, Börner J, Liebig A, Albrecht M, Kloc C, Gordan O and Zahn D R 2013 *Opt. Express* **21** 4908–16
[4] Chhowalla M, Shin H S, Eda G, Li L-J, Loh K P and Zhang H 2013 *Nat. Chem.* **5** 263–75
[5] Wang Q H, Kalantar-Zadeh K, Kis A, Coleman J N and Strano M S 2012 *Nat. Nanotechnol.* **7** 699–712
[6] Yan Z, Chen L, Yoon M and Kumar S 2016 *ACS Appl. Mater. Interfaces* **8** 33299–306
[7] Zhang Y, Chang T-R, Zhou B, Cui Y-T, Yan H, Liu Z, Schmitt F, Lee J, Moore R and Chen Y 2014 *Nat. Nanotechnol.* **9** 111–5
[8] Tongay S, Zhou J, Ataca C, Lo K, Matthews T S, Li J, Grossman J C and Wu J 2012 *Nano Lett.* **12** 5576–80
[9] Late D J, Shirodkar S N, Waghmare U V, Dravid V P and Rao C 2014 *ChemPhysChem* **15** 1592–8
[10] Horzum S, Sahin H, Cahangirov S, Cudazzo P, Rubio A, Serin T and Peeters F 2013 *Phys. Rev.* B **87** 125415
[11] Onga M, Zhang Y, Suzuki R and Iwasa Y 2016 *Appl. Phys. Lett.* **108** 073107
[12] Chang Y-H, Zhang W, Zhu Y, Han Y, Pu J, Chang J-K, Hsu W-T, Huang J-K, Hsu C-L and Chiu M-H 2014 *ACS Nano* **8** 8582–90
[13] Bernardi M, Palummo M and Grossman J C 2013 *Nano Lett.* **13** 3664–70
[14] Larentis S, Fallahazad B and Tutuc E 2012 *Appl. Phys. Lett.* **101** 223104
[15] Kumar S and Schwingenschlogl U 2015 *Chem. Mater.* **27** 1278–84
[16] Shafique A and Shin Y-H 2017 *Sci. Rep.* **7** 506
[17] Gu X and Yang R 2014 *Appl. Phys. Lett.* **105** 131903
[18] Peng B, Zhang H, Shao H, Xu Y, Zhang X and Zhu H 2016 *RSC Adv.* **6** 5767–73
[19] Li W, Carrete J and Mingo N 2013 *Appl. Phys. Lett.* **103** 253103
[20] Slack G A 1973 *J. Phys. Chem. Solids* **34** 321–35
[21] Morelli D and Heremans J 2002 *Appl. Phys. Lett.* **81** 5126–8
[22] Lin J, Pantelides S T and Zhou W 2015 *ACS Nano* **9** 5189–97
[23] Zhang K, Feng S, Wang J, Azcatl A, Lu N, Addou R, Wang N, Zhou C, Lerach J and Bojan V 2015 *Nano Lett.* **15** 6586–91
[24] Li X *et al* 2017 *Adv. Funct. Mater.* (https://doi.org/10.1002/adfm.201770119)
[25] Mahjouri-Samani M, Liang L, Oyedele A, Kim Y-S, Tian M, Cross N, Wang K, Lin M-W, Boulesbaa A and Rouleau C M 2016 *Nano Lett.* **16** 5213–20
[26] Gong Y, Liu Z, Lupini A R, Shi G, Lin J, Najmaei S, Lin Z, Elías A L, Berkdemir A and You G 2013 *Nano Lett.* **14** 442–9
[27] Azizi A, Zou X, Ercius P, Zhang Z, Elías A L, Perea-López N, Stone G, Terrones M, Yakobson B I and Alem N 2014 *Nat. Commun.* **5** 4867
[28] Peng B, Ning Z, Zhang H, Shao H, Xu Y, Ni G and Zhu H 2016 *J. Phys. Chem.* C **120** 29324–31
[29] Ding Z, Pei Q-X, Jiang J-W and Zhang Y-W 2015 *J. Phys. Chem.* C **119** 16358–65
[30] Han H-V, Lu A-Y, Lu L-S, Huang J-K, Li H, Hsu C-L, Lin Y-C, Chiu M-H, Suenaga K and Chu C-W 2016 *ACS Nano* **10** 1454–61
[31] Lin Z, Carvalho B R, Kahn E, Lv R, Rao R, Terrones H, Pimenta M A and Terrones M 2016 *2D Mater.* **3** 022002
[32] Lin Z, McCreary A, Briggs N, Subramanian S, Zhang K, Sun Y, Li X, Borys N J, Yuan H and Fullerton-Shirey S K 2016 *2D Mater.* **3** 042001
[33] Azizi A, Wang Y, Stone G, Elias A L, Lin Z, Terrones M, Crespi V H and Alem N 2017 *Nano Lett.* **17** 2802–8
[34] Li X, Lin M-W, Puretzky A A, Basile L, Wang K, Idrobo J C, Rouleau C M, Geohegan D B and Xiao K 2016 *J. Mater. Res.* **31** 923–30
[35] Azizi A, Wang Y, Lin Z, Wang K, Elias A L, Terrones M, Crespi V H and Alem N 2016 *Nano Lett.* **16** 6982–7
[36] Li X, Lin M W, Basile L, Hus S M, Puretzky A A, Lee J, Kuo Y C, Chang L Y, Wang K and Idrobo J C 2016 *Adv. Mater.* **28** 8240–7
[37] Kresse G and Furthmüller J 1996 *Phys. Rev.* B **54** 11169
[38] Perdew J P 1986 *Phys. Rev.* B **33** 8822–4
[39] Kresse G and Joubert D 1999 *Phys. Rev.* B **59** 1758
[40] Perdew J P, Burke K and Ernzerhof M 1996 *Phys. Rev. Lett.* **77** 3865
[41] Böker T, Severin R, Müller A, Janowitz C, Manzke R, Voß D, Krüger P, Mazur A and Pollmann J 2001 *Phys. Rev.* B **64** 235305
[42] Maradudin A and Fein A 1962 *Phys. Rev.* **128** 2589
[43] Wu X, Lee J, Varshney V, Wohlwend J L, Roy A K and Luo T 2016 *Sci. Rep.* **6** 22504
[44] Li W, Carrete J, Katcho N A and Mingo N 2014 *Comput. Phys. Commun.* **185** 1747–58
[45] Broido D, Malorny M, Birner G, Mingo N and Stewart D 2007 *Appl. Phys. Lett.* **91** 231922
[46] Matthiessen A and Vogt C 1864 *Phil. Trans. R. Soc.* **154** 167–200
[47] Li W, Lindsay L, Broido D, Stewart D A and Mingo N 2012 *Phys. Rev.* B **86** 174307
[48] Nika D, Pokatilov E, Askerov A and Balandin A 2009 *Phys. Rev.* B **79** 155413
[49] Ratsifaritana C and Klemens P 1987 *Int. J. Thermophys.* **8** 737–50
[50] Klemens P and Pedraza D 1994 *Carbon* **32** 735–41
[51] Klemens P 1955 *Proc. Phys. Soc.* A **68** 1113
[52] Xie G, Shen Y, Wei X, Yang L, Xiao H, Zhong J and Zhang G 2014 *Sci. Rep.* **4** 5085
[53] Lindsay L, Broido D and Reinecke T 2013 *Phys. Rev. Lett.* **111** 025901